International Journal of Remote Sensing
Vol. 32, No. 24, 20 December 2011, 9343–9363

Taylor & Francis
Taylor & Francis Group

Three-point observation in the troposphere over Sofia-Plana Mountain, Bulgaria

Ts. T. EVGENIEVA†, B. L. B. WIMAN‡, N. I. KOLEV†, P. B. SAVOV§, E. H. DONEV¶, D. I. IVANOV¶, V. DANCHOVSKI¶, B. K. KAPRIELOV†, V. N. GRIGORIEVA†, I. Ts. ILIEV| and I. N. KOLEV*†

†Institute of Electronics, Laser Radars Laboratory, Bulgarian Academy of Sciences, Sofia, Bulgaria

‡Environmental Science and Technology Section, Linnaeus University, Kalmar, Sweden

§Department of Physics, University of Mining and Geology 'St. Ivan Rilski', Sofia, Bulgaria

¶Department of Meteorology and Geophysics, Faculty of Physics, Sofia University 'St. Kliment Ohridsky', Sofia, Bulgaria

|Central Laboratory of Solar-Terrestrial Influences, Bulgarian Academy of Sciences, Sofia, Bulgaria

(*Received 15 December 2009; in final form 3 January 2011*)

Based on a novel combination of approaches and instruments, this article presents campaign-based results from atmospheric boundary layer (ABL) height and aerosol optical depth (AOD) measurements carried out at two different experimental sites in Sofia, as well as from three-point measurements of aerosol number concentrations. Several instruments (lidar (developed by the IE), ceilometer, aerosol particle counter, sun photometer and meteorological sensors) were used in this study. Based on joint interpretation of the instruments' data we assess the influence of the atmospheric aerosol in the planetary boundary layer and the significant influence of aerosol layers and high clouds on AOD values. Measurements of AOD in the city basin gave values in the range 0.22–0.41 for cloud-free skies, and up to around 0.8 under partly cloudy conditions. The information obtained during the two campaigns indicates that aerosol particle concentrations were lower in park areas than along heavy-traffic thoroughfares in the city, but higher than in the mountain area. In conclusion, our study demonstrates the potential of employing a broad array of instruments for the study of boundary layer and aerosol over large, valley-situated and heavily urbanized city areas.

1. Introduction

The atmospheric boundary layer (ABL) is an important element of the Earth's climate system. The exchange of heat, momentum, moisture, aerosol and gaseous components between the Earth's surface and the free troposphere occurs in the ABL. The processes involved determine the structure of the low atmosphere, pollutant dispersal over complex terrain and the formation of stratocumulus and cumulus clouds (Kondratyev and Varotsos 1995, Hongbin *et al*. 2002, Fenger 2009).

*Corresponding author. Email: blteam@ie.bas.bg; evgenieva@mail.bg

International Journal of Remote Sensing
ISSN 0143-1161 print/ISSN 1366-5901 online © 2011 Taylor & Francis
http://www.tandf.co.uk/journals
http://dx.doi.org/10.1080/01431161.2011.554456

The ABL height is often identified with the height of the mixing layer (ML), one of the most important parameters governing the concentration and dispersion of trace gases and aerosol particles (Varotsos *et al*. 1995, Katsambas *et al*. 1997, Varotsos *et al*. 2001a, Gerasopoulos *et al.* 2005, Kolev *et al.* 2007, Evgenieva *et al.* 2009). Hence, assessments of the ABL height are fundamental to environmental monitoring, weather forecasting and air pollution research (Jacovides *et al.* 1994, Seibert *et al.* 2000, Jacob and Winner 2009).

ABL research follows several routes. Some investigations are being aimed at equalizing methods to determine ABL heights, including through remote sensing (radars, sodars, lidars) (Beyrich *et al.* 1996a, Kolev *et al.* 2004, McKendry *et al.* 2009) for use in meteorological applications (Seibert *et al.* 2000, Kondratyev and Varotsos 2002, Grimmod 2006).

Another significant scope of ABL investigations is the study of air pollution over big cities. Substances emitted into the ABL are gradually dispersed horizontally and vertically through the action of the turbulence, and finally become completely mixed across this layer (Jacovides *et al.* 1994, Ferm *et al.* 2005, 2006, Alfoldy *et al.* 2007, Chou *et al.* 2007, Kolev *et al.* 2007).

One new direction of ABL investigations is the use of models to help assess the influence of the processes in the ABL on the global climate. Of particular interest are the relations between different local models and general circulation models (GCMs) (Medeiros *et al.* 2005). Some such research attempts to account for the influence of the atmospheric aerosol, mainly in the ABL and free atmosphere, on the ABL development and on meteorological characteristics. For instance, solar radiation, relative humidity, temperature and soil moisture are then studied in relation to aerosol optical characteristics such as scattering, absorption and single scattering albedo (Hongbin *et al.* 2002, Markowitcz *et al.* 2003, Alados-Arboledas *et al.* 2008, Tzanis and Varotsos 2008).

The height of the ABL determines the volume wherein air pollutants are spread and subject to physico-chemical transformations. Over an urban area, most of the aerosol resides within the first 2–3 km (by height) of the atmosphere (Kolev *et al.* 2007). The atmospheric aerosol is of fundamental importance to our understanding of climate change (e.g. Intergovernmental Panel on Climate Change (IPCC) 2007), ecological problems (e.g. Reinap *et al.* 2009), ground-near ozone dynamics (e.g. Seinfeld and Pandis 1998), human health (Houthuijs *et al.* 2001) and the many atmospheric dynamics issues involved (Markowitcz *et al.* 2003, Kolev *et al.* 2004, Evgenieva *et al.* 2009, Fenger 2009).

Of particular interest in this context are studies in megacities, such as the long-term (over 15 years) research in Mexico City by Velasco *et al*. (2008), and in urbanized regions in Europe, including the Balkan Peninsula (Cartalis and Varotsos 1994, Beyrich *et al.* 1996a,b, Varotsos *et al.* 2001a,b) and Iberian Peninsula (Lyamani *et al.* 2004, 2005, 2006a, b, 2008, Sicard *et al.* 2006, Alados-Arboledas *et al.* 2008, Guerrero-Rascado *et al.* 2009). Velasco *et al*. (2008), using a tethered balloon to investigate spatial distributions of zone and volatile organic compounds (VOCs), showed that ozone concentration reaches maximum values around 12–15 hours local standard time (LST) and fluctuates around these values during the development of the ML. Beyrich *et al.* (1996a,b), in two experimental campaigns in the Harz Mountains and Upper Rhine Valley, deployed sodar, ground-based meteorological stations and a tethered balloon with lightweight sensors in order to study ozone concentrations during the formation of the ML.

A range of studies have addressed the influence of the sun radiation on ozone concentration, estimating the influence of the meteorological components (temperature, relative humidity, wind speed) (Chandra and Varotsos 1995, Gernandt *et al.* 1995, Varotsos *et al.* 2001b, 2004, Varotsos 2004, Gerasopoulos *et al.* 2005).

During the Veleta summer 2002 campaign, in the Sierra Nevada Mountains close to Granada in southeastern Spain, four Cimel CE-318 robotic radiometers were placed at four different altitudes (Alados-Arboledas *et al.* 2008). Changes in the spectral dependence of the single scattering albedo under different air masses were assessed. This enabled a detailed study of the columnar aerosol properties at different locations during the formation of the ABL.

Based on a pure scientific interest as well as on the ecological problems in the big cities and the decisions taken in Paris on 2 February 2007 when the Working Group I of the IPCC adopted the Summary for Policymakers of the first volume of 'Climate Change 2007', also known as the Fourth Assessment Report (AR4) (Cracknell and Varotsos 2007), we have extended our investigation of the atmospheric aerosol in the ABL as well as in whole tropospheric layer and also of the behaviour of the ground-near ozone concentration at two different heights. Our ambition is to build up a base for up-to-date control of the atmospheric pollutant and its influence on local climate and, from the other side, to add another point to the regular observations of the atmosphere.

The objective of this article is to determine optical and microphysical characteristics of the atmospheric aerosol in the heavily urbanized mountain valley hosting Sofia city, and the variation of these characteristics during the ABL formation. To this end, we present results from combined campaign measurements using lidar, ceilometer, sun photometer, aerosol particle counter and meteorological sensor equipment. Measurements were at three locations: in a residential area close to traffic thoroughfares, in a park zone and at a station in the Plana Mountain area above the city valley (cf. figure 1). Our article should be seen in the broader context of our long-term lidar observations on aerosol structure of the ABL in the valley of Sofia (Kolev *et al.* 2000, Savov *et al.* 2002, Evgenieva *et al.* 2009), where lidar data have helped to provide a detailed picture of the processes in the planetary boundary layer (up to 2000 m) and of the structure, height and lifetime of the different strata in the ABL (Kolev *et al.* 2004, 2007, Evgenieva *et al.* 2009). An additional contextual basis is constituted by the long-term meteorological observations, including ground-near ozone concentrations, in the regions of Rozhen, Ahtopol, Sofia and Plana carried out by Donev *et al*. (2002), and by several sequences of aerosol sampling and physico-chemical aerosol characterizations at various sites in Bulgaria (Wiman *et al.* 2007).

2. Theoretical background

The following lidar equation, under the assumption of single scattering (Collis and Russell 1976), was used to process the lidar data:

$$P(z) = P_0 K_{\mathrm{L}} \beta_\pi z^{-2} \exp\left\{-2\int_0^z \sigma(z)\mathrm{d}z\right\}, \tag{1}$$

where $P(z)$ is the received backscattered light power; P_0 is the transmitted laser light power; K_{L} is a constant characteristic of each lidar system and depends on the technical specifics of the lidar's emitting and receiving optics; β_π is the atmospheric aerosol

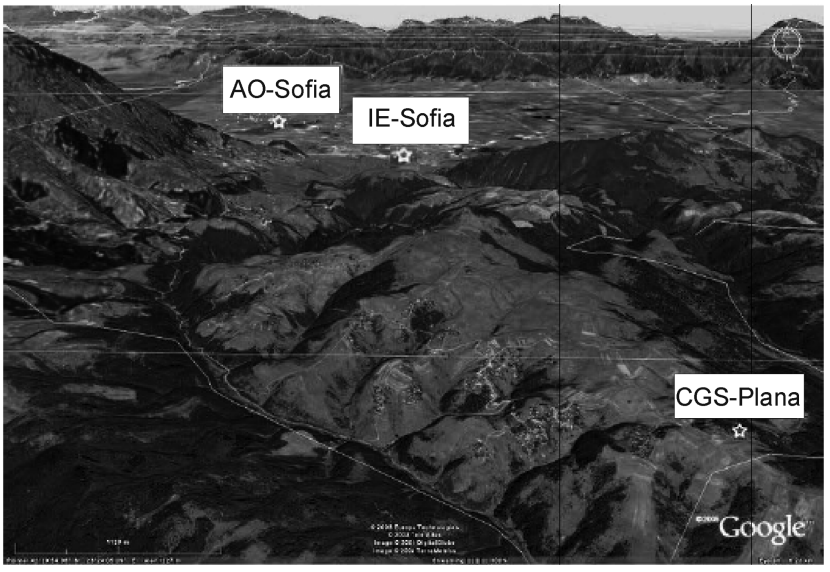

Figure 1. An overview of the Sofia plus Plana region. AO, Astronomical Observatory; IE, Institute of Electronics; CGS, Central Geophysical Station
(Source: Google © 2008 Europa Technologies, © 2008 Tele Atlas. Image © 2008 DigitalGlobe, Image © 2008 Terrametrics).

backscattering coefficient; z is the distance from the lidar along the sounding path; and $\sigma(z)$ is the extinction coefficient.

The method for aerosol optical depth (AOD) determination is based on the Beer–Lambert–Bouguer law (Devara *et al.* 1996):

$$E_\lambda = \left(\frac{E_{0\lambda}}{R^2}\right) \exp\{-m\tau_\lambda^{\text{tot}}\}, \tag{2}$$

where E_λ is the solar radiation measured at the Earth's surface at a particular wavelength λ; $E_{0\lambda}$ is the solar radiation at the top of the atmosphere (calibration constant) at that wavelength; R is the Earth–Sun distance in astronomical units; m is the relative air mass which is approximated as the secant of the solar zenith angle and $\tau_\lambda^{\text{tot}}$ is the total optical depth (TOD) at a particular wavelength λ. The TOD is the sum of AOD τ_λ^{a}, Rayleigh scattering optical depth τ_λ^{r}, optical depth of gaseous absorption τ_λ^{g} and optical depth of water vapour $\tau_\lambda^{\text{H}_2\text{O}}$. Once the TOD is obtained one can determine the AOD at a particular wavelength from the following expression:

$$\tau_\lambda^{\text{a}} = \tau_\lambda^{\text{tot}} - \tau_\lambda^{\text{r}} - \tau_\lambda^{\text{g}} - \tau_\lambda^{\text{H}_2\text{O}}. \tag{3}$$

After the AOD is obtained its dependence on wavelength can be analysed using the Ångström formula (Martinez-Lozano *et al*. 1998):

$$\tau_\lambda^{\text{a}} = \beta\lambda^{-\alpha}, \tag{4}$$

where λ is the wavelength expressed in micrometres; β is the aerosol extinction coefficient corresponding to the wavelength of 1 μm ('the Ångström turbidity coefficient',

reflecting the aerosol particle concentration and thus relating to air pollution status); and α is 'the Ångström exponent' (reflecting the distribution of particle number concentration as a function of particle size).

3. Sites and instruments

The ground-based aerosol lidar was placed at the Laser–Radar Laboratory of the Institute of Electronics (IE). The ceilometer (CHM 15k), sun photometer (Microtops II, Solar Light Company, Philadelphia, PA, USA), laser-based aerosol particle counter (LPC, a portable HHPC-6 instrument, Hach Ultra Analytics SA, Switzerland) and meteorological station (which includes a TECO ozonemeter, Thermo Environmental Instruments Inc., Franklin, MA, USA) were placed at the Astronomical Observatory (AO) of the Sofia University 'St. Kliment Ohridsky', Borisova Gradina Park at a distance of about 300 m away from Tsarigradsko Shosse Blvd. The LPC was also used in residential and traffic areas in Sofia and at locations along the mountain up to and at the Central Geophysical Station (CGS) in the Plana Mountain (see figure 1). Another meteorological station (also including a TECO ozonemeter) was located at the CGS site. The main parameters of the five devices are as follows.

Specifications of the lidar
Transmitter: a standard Nd-YAG (neodymium-doped yttrium aluminium garnet, $Nd:Y_3Al_5O_{12}$) laser (operational wavelength: 532 nm; pulse duration and energy: 15–20 ns and 10–15 mJ; repetition rate: 12.5 Hz; receiving antenna consists of a Cassegrain telescope with main mirror diameter of 150 mm and equivalent focal length of 2250 mm); photodetector: a photomultiplier tube (PMT) with an interference filter 1 nm full width at half maximum (FWHM); data acquisition and processing set: a 10 bit 20 MHz analog-to-digital converter (ADC) and a PC. The lidar overlap altitude is 75 m (Kolev *et al.* 2004).

Specifications of the sun photometer
Optical channels: $\lambda = 380$ nm, $\lambda = 500$ nm, $\lambda = 675$ nm, $\lambda = 936$ nm and $\lambda = 1020$ nm; viewing angle: 2.5°; dynamic range: $> 3 \times 10^5$; computer interface RS232, data storage: 800 records; power source: $4 \times$ AA alkaline batteries.

Specifications of the ceilometer
Light source: laser protection class 1M under DIN EN 60825-1; measuring range: 30–15 000 m; resolution: 15 m; measuring time: 60 s; measuring principle: optical (lidar) with photon counting (24 hours continuous operation); wavelength: 1064 nm; pulse duration: about 1 ns; pulse repetition rate: 5–7 kHz; energy per pulse: 8 μJ. The commercial ceilometer CHM 15k is manufactured by Jenoptik Laser, Optik, Systeme GmbH, Germany.

Specifications of the LPC
LPC samples and classifies aerosol particles into six particle size ranges (geometric particle diameter: 0.3–0.5, 0.5–0.7, 0.7–1, 1–2, 2–5 and >5 μm) giving output data in terms of number of particles per litre of air samples. The LPC is portable, has a sampling flow rate of 2.83 l m^{-1} and can be programmed in various manners (Wiman *et al.* 2007).

Specifications of the meteorological stations

Both stations hold sensors, at 10 m above ground, for measuring total solar radiation (SP1110 Skye Pyranometer, Campbell Scientific Ltd., Loughborough, UK), wind speed and wind direction (05103 YOUNG monitor, R. M. Young Company, Traverse City, MI, USA); sensors, at 2 m above ground, for air temperature and relative humidity (Vaisala HMP45C, Vaisala Ltd., Birmingham, UK); and sensors, at 0.5 m, for measuring precipitation (MRI). Ozone concentrations at 1.5 m above ground were measured at both stations with TECO 49 instruments (ultraviolet (UV) photometer principle is based on the attenuation of light due to ozone in the absorption cell at a wavelength of 254 nm). Due to the inherent stability of the UV absorption technique used, the ozone concentrations reported here are within ±5 ppb (by volume). Hourly mean and SDs of the measured quantities were recorded (at 0.1 Hz sampling rate) using a Campbell Scientific CR10X data logger (Campbell Scientific Ltd., Loughborough, UK) (Donev *et al.* 2002).

4. Experimental results

Two campaigns were carried out, one in late summer 2008 and one in spring 2009. This project is based on the idea of comparing various air quality aspects pertaining to the Sofia city 'basin' with those pertaining to surrounding mountain areas (Kolev *et al.* 2007, Evgenieva *et al.* 2009). An overview of the Sofia city plus Plana region is shown in figure 1. The locations of the IE, Sofia (42.39° N, 23.23° E, 591 m above sea level); the AO, Sofia (577 m above sea level); and the Plana Mountain CGS (1239 m above sea level) are marked by asterisks.

4.1 *Lidar, sun photometer and LPC data (summer campaign 2008)*

As lidar remote sensing makes use of the aerosol as a passive tracer, the power of the received signal is proportional to the size, shape, concentration and wetting of aerosol particles. During lidar observations, 6000 profiles were recorded during a period of about 9–10 minutes. Consecutive profiles were averaged with respect to the number of shots (150) to increase the signal-to-noise ratio; the 40 profiles thus obtained were then transformed into *S*-functions. The results of the lidar observations are presented as height–time indicators/images (HTI) of the *S*-functions of the lidar signals calculated for each point of the sounding path. The *S*-function is used instead of the lidar return itself since it reveals the aerosol structure of the atmosphere much better. The *S*-function is commonly defined as $S = r^2 \ln P$, where P is the received backscattered light power and r is the distance from the lidar along the sounding path (it is well known that the lidar return decreases as the inverse square of the distance r) (Kolev *et al.* 2007).

Figure 2 shows results of the lidar experiment that was commenced on 5 September 2008 at 08:05 LST and finished at 13:00 LST. In the beginning of the experiment a stable boundary layer (SBL) at a height of about 250 m was observed. The new ML began to form around 09:30–10:00 LST, reaching a height of 350 m at 10:30 LST and a height of 600 m at 12:00 LST and remained at this height until the end of the experiment (13:00 LST).

Sun photometer data obtained on 5 September 2008 at the AO site are shown in figure 3. The measurements started at 12:30 LST and had to be finished at 14:30 LST due to atmospheric conditions (presence of clouds) unsuitable for this kind of measurement. Some clouds began to appear after 12:45 LST, as reflected by the AOD value of 0.7 at 13:05 LST. The influence of clouds decreased around

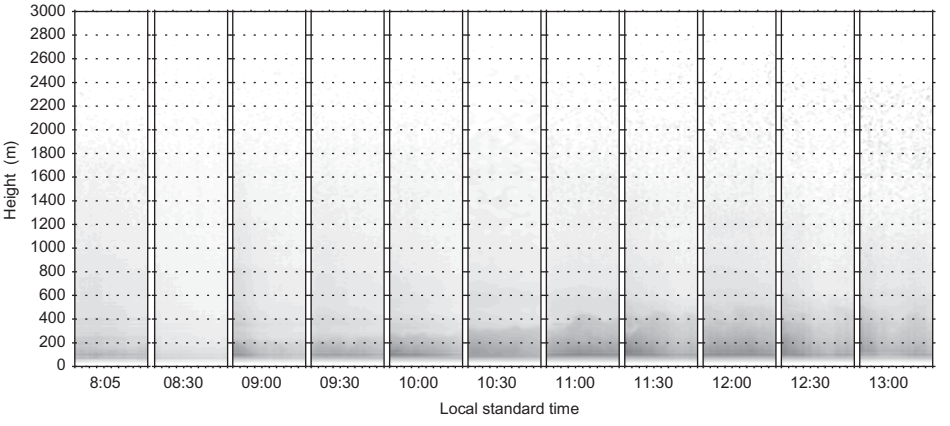

Figure 2. Range-corrected signals constructed from the lidar data obtained on 5 September 2008 at the Institute of Electronics, Sofia.

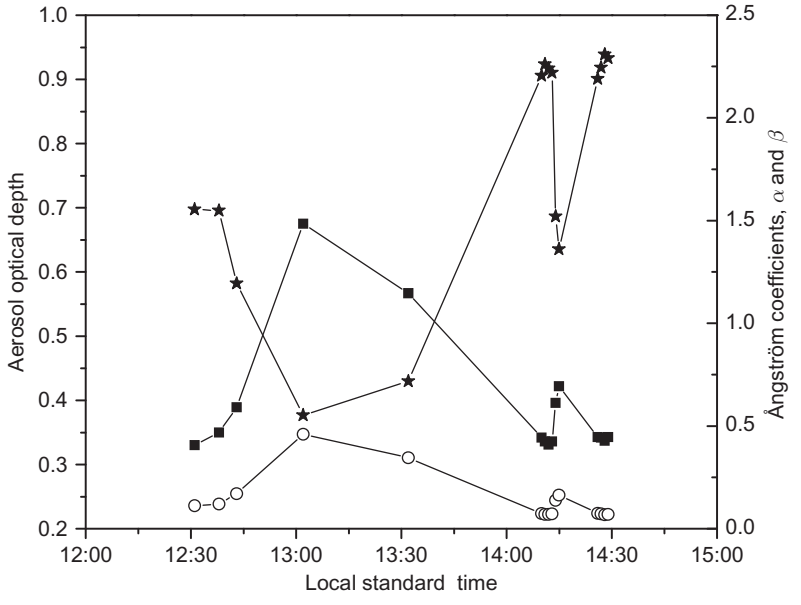

Figure 3. Daily variation of the aerosol optical depth (filled squares) and Ångström coefficients (stars, α; unfilled circles, β) obtained by sun photometer on 5 September 2008 at the AO, Sofia.

14:15 LST, with AOD decreasing towards the value of 0.35 in the beginning of the experiment. After 14:15 LST the clouds became denser and the measurements were stopped.

In figure 4 an attempt to explore how particle number concentrations vary with altitude in the Sofia city versus Plana Mountain region is shown. Because only a sequential measuring strategy could be employed, interpretations need some caution. The diagram shows that particle number concentrations (in the size range 0.3–1 μm) decreased en route from the city basin and upwards during the morning travel (by car) to the Plana site. At that site, concentrations were almost a factor 2 lower than in the

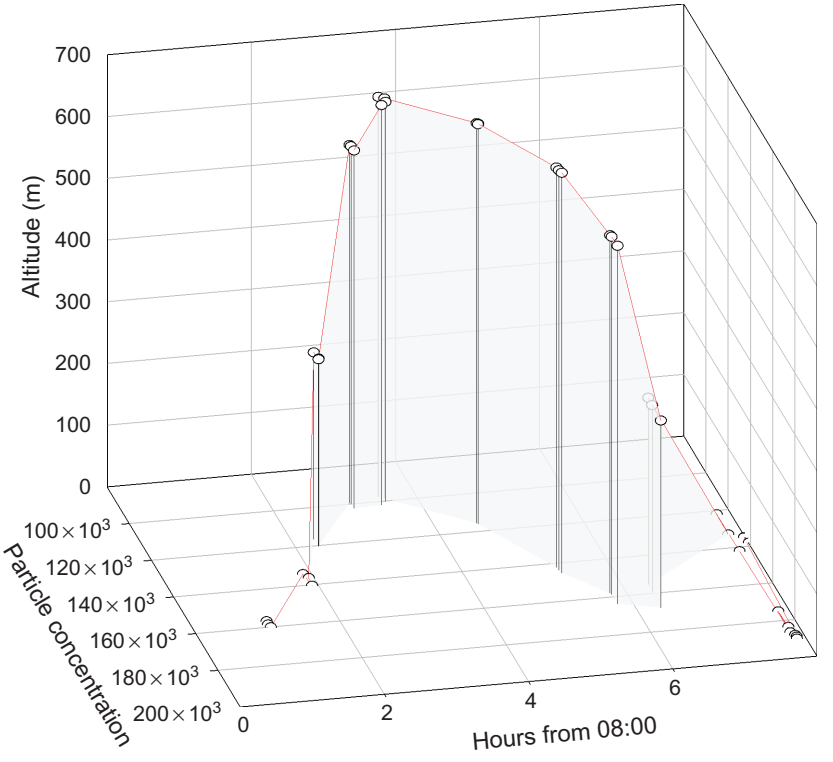

Figure 4. Particle concentration (number of particles in size range 0.3–1 μm l^{-1}) in relation to altitude above Sofia basin and time of day (Greenwich Mean Time (GMT)+3). Measurements carried out on 3 September 2008 en route from the city basin and upwards at different sites during travel to the Plana site, at the Plana site and en route downwards back to the Sofia basin.

basin. However, during the continued course of measurements in the Plana region, concentrations began to rise. En route downwards back to the Sofia basin, concentrations continued to rise, although after some time in the Sofia basin concentrations first declined somewhat and then again increased. The diagrams of particle size distribution (not shown here) suggest that the estimated volume versus size distributions were quite different in Sofia city and at Plana site. Although both distributions tend to be bimodal (cf. Whitby (1978)), the coarse particle volume mode (particle sizes > 2 μm) is much larger than the accumulation volume mode (particle sizes in the range from $\sim$0.1 to $\sim$2 μm) in strongly active city area, whereas the accumulation volume mode dominates at the mountain site.

4.2 *Ceilometer, lidar, sun photometer and LPC data (spring campaign 2009)*

The ceilometer CHM 15k was located at the AO site (in the Borisova Gradina Park) at a distance of about 7 km from the IE. As a result of the specifics of the ceilometer (see §3) data were obtained in the height range from 30 to 15 000 m, that is, from substantially higher altitudes than those reachable with the lidar. For the scope of this article we confine our discussion of ceilometer data to those pertinent to the ABL and heights up to 4000 m. We observe that the longer wavelength of the ceilometer

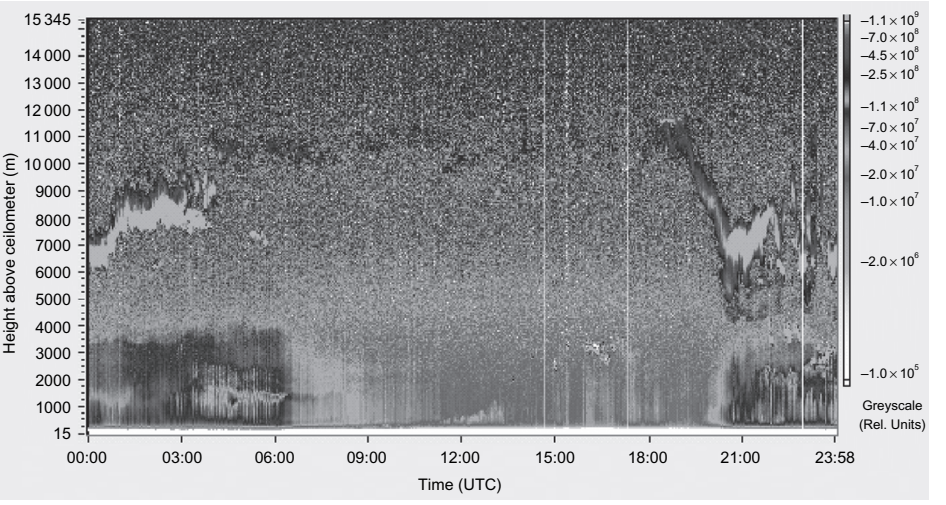

Figure 5. Range-corrected signals constructed from the ceilometer CHM 15k data obtained on 15 May 2009 at the Astronomical Observatory, Sofia. The grey scale represents the lidar signal in relative units.

(1064 nm) in relation to that of the lidar (532 nm) implies a higher sensitivity to the influence of relative humidity on the atmospheric aerosol.

The ceilometer data from 15 May 2009 are shown in figure 5. Three layers were observed in the lower part of the troposphere at heights $H_1 = 1500$ m, $H_2 = 2500$ m and $H_3 = 3500$ (up to 3750) m. Two layers at heights $H_1 = 1500$ m and $H_2 = 2000$ m were clearly identifiable after 07:00 LST. The mixing layer height (MLH) was between 250 and 400 m up to 11:00 LST, at 13:30 LST MLH was 1500 m, increasing to 2500 m at 15:00 LST. Between 07:00 and 13:30 LST clouds (Cirrus type) were observed at around 10 000–11 000 m, probably reducing the solar radiation reaching the Earth's surface.

Figure 6 shows the ceilometer data obtained on 22 May 2009. The experiment started at 00:00 LST and finished at 23:58 LST, and enabled us to follow the temporal development of the SBL, the residual layer (RL) and the convective boundary layer (CBL). Over the first 3 hours the SBL at a height of 200 m remained from the previous night. Also observable in figure 6 are RLs divided into two parts, the first one at a height of 1000 m and the second one at a height of 2000 m. The residual layer height (RLH) decreased constantly and the RL is fully destroyed at 13:30 LST. The new ML starts to form around 09:30 LST and gradually and constantly increases up to about 1000 m at 12:00 LST, and at 15:00 LST the MLH is about 2000 m.

In the ceilometer data a layer is observed which is located above the RL and reaches a height of about 3000 m and in particular cases 4000 m. During the experiments, the height of the SBL reaches 200 m but is not very well defined. The RLH is in the range from 1500 to 2000 m. The MLH reaches 2000–2250 m around 15:00 LST, that is, about 1–1.5 hours later than the lidar data shown (cf. figure 7). The ceilometer enabled observation of the formation of the atmospheric nocturnal stratification after sunset.

Aerosol lidar results from 15 May 2009 are shown in figure 7. The experiment started at 07:04 LST and ended at 13:30 LST. Lidar data obtained show a non-typical development of SBL and RL in the period from 07:04 to 10:30 LST. After 11:00 LST,

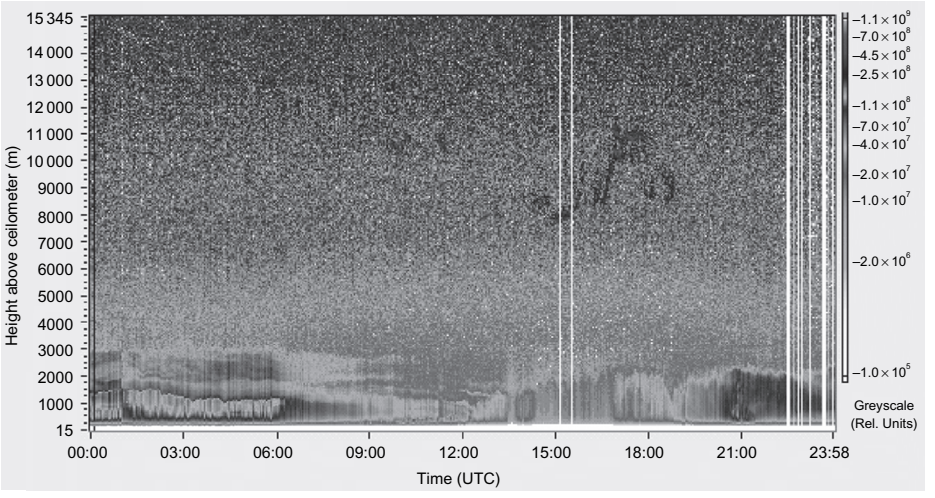

Figure 6. Range-corrected signals constructed from the ceilometer CHM 15k data obtained on 22 May 2009 at the Astronomical Observatory, Sofia. The grey scale represents the lidar signal in relative units.

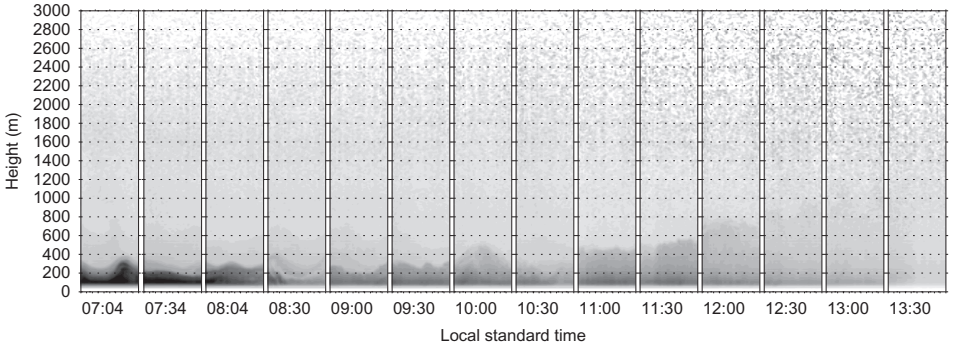

Figure 7. Range-corrected signals constructed from the lidar data obtained on 15 May 2009 at the Institute of Electronics, Sofia.

RL was destroyed and a gradual increase in the height of the ML began. MLH reached 1000 m at 12:30 LST and 1600–1800 m at 13:30 LST. A possible reason for the ABL behaviour in the morning hours could be the changing amount of solar radiation reaching the Earth's surface.

In figure 8, aerosol lidar data obtained on 21 May 2009 are shown. The measurements were performed from 07:25 to 13:30 LST. On the 07:25 LST lidar image, an aerosol layer at about 200 m is observable; this is the SBL. The second layer at around 1200–1400 m height is the RL remaining from the previous day. On the second image two layers can be seen. At 10:30 LST the ML reached the height of 1000 m and destroyed the RL at this height. According to the lidar data, an aerosol layer with higher humidity resided at about 1200 m at 11:00 LST. Later, this can be seen on the image at 12:00 LST, showing a layer at 1600 m, above the ML. At 12:30 LST the ML reaches 1600 m. At 13:00 LST the upper border of the ML is about 2000 m.

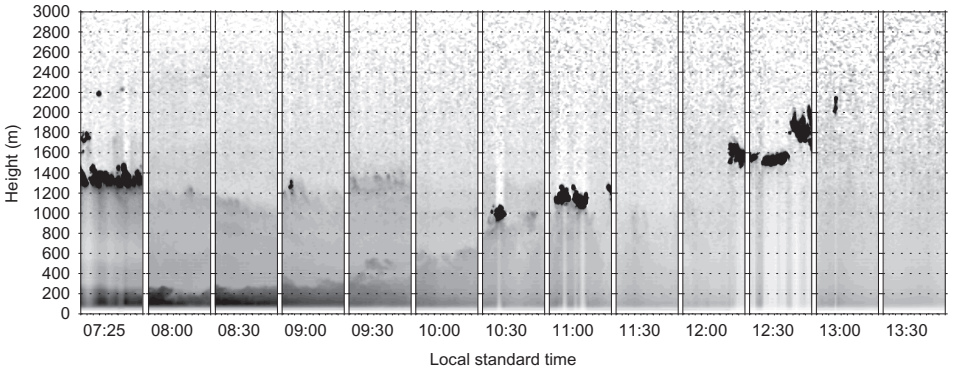

Figure 8. Range-corrected signals constructed from the lidar data obtained on 21 May 2009 at the Institute of Electronics, Sofia.

In summary, the lidar data for the whole period of experiments from 12 May 2009 to 26 May 2009 show the following: during all days the SBL height was in the range from 200 to 300 m and existed until 08:30–09:30 LST. RLH varied from 1400 m on 21 May 2009 to between 2000 and 2200 m on 12 May 2009 and 19 May 2009. The RL was fully destroyed in the period between 11:00 and 13:00 LST. The ML began to gradually increase between 08:30 and 11:30 LST, whereupon a rapid increase in the ML height occurred, and around 13:00 LST MLH reached about 1800–2200 m. The rapid differential increase in the ML height usually was in the range 400–600 m.

The sun photometer was located next to the ceilometer at the AO site in the period 19 May 2009–22 May 2009 (figures 9 and 10). The experimental AOD data obtained at $\lambda = 500$ nm can be summarized as follows. The AOD varied in the range 0.22–0.41 under clear sky conditions. When clouds were present, AOD reached values of 0.74–0.80. The height of the cloud base according to ceilometer data was in the range 8–11 km. Roughly, two main temporal regions can be separated in the AOD behaviour. The first one is characterized by fairly large variations in AOD values, and is from the beginning of the experiments (both starting at around 09:30 LST) until about 11:30 LST. The second region stretches from 12:00 to 15:00 LST when AOD was almost constant. The only case when AOD gradually increased after 12:00 LST from 0.30 to 0.41 is during the experiment on 19 May 2009 which could be due to long-range advection from other pollutant sources.

Figure 11 shows the data from the aerosol particle counter measurements carried out at three experimental sites in the period between 16 May 2009 and 23 May 2009: an urban residential area site (next to a traffic thoroughfare, Tsarigradsko Shosse Blvd.), the AO park site and the CGS site in the Plana Mountain. The data can be summarized as follows. The aerosol concentration in the particle size range 0.3–1 μm varied from 40 000 to 150 000 l^{-1}. The lowest concentrations were usually observed around noon (when the ML is developed) for the three experimental sites. The highest concentrations were measured in the residential area during morning and afternoon traffic jam hours.

4.3 *Meteorology during the experiments*

Solar radiation measured at the CGS (Plana Mountain) and AO (Borisova Gradina Park) sites on 21 May 2009 is presented in figure 12, and the behaviour of ground-near

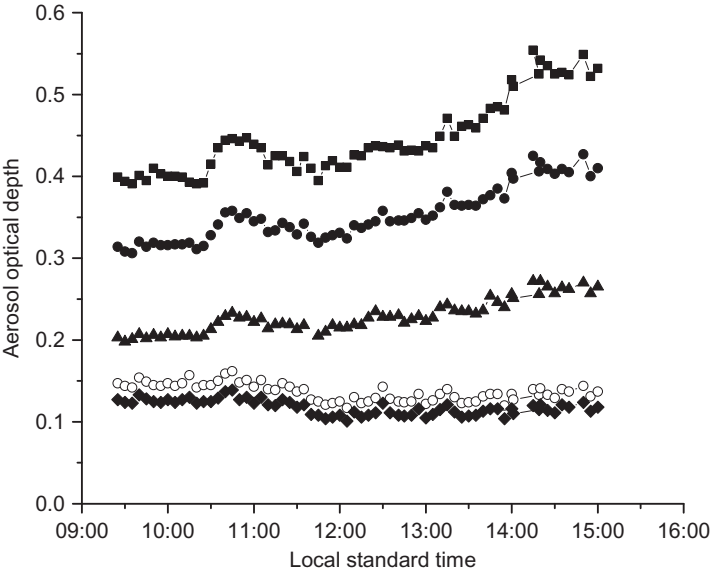

Figure 9. Daily variation of the aerosol optical depth at wavelengths $\lambda = 380$ nm (squares), $\lambda = 500$ nm (filled circles), $\lambda = 675$ nm (filled triangles), $\lambda = 936$ nm (unfilled circles) and $\lambda = 1020$ nm (filled rhombs) obtained by sun photometer on 19 May 2009 at the Astronomical Observatory, Sofia.

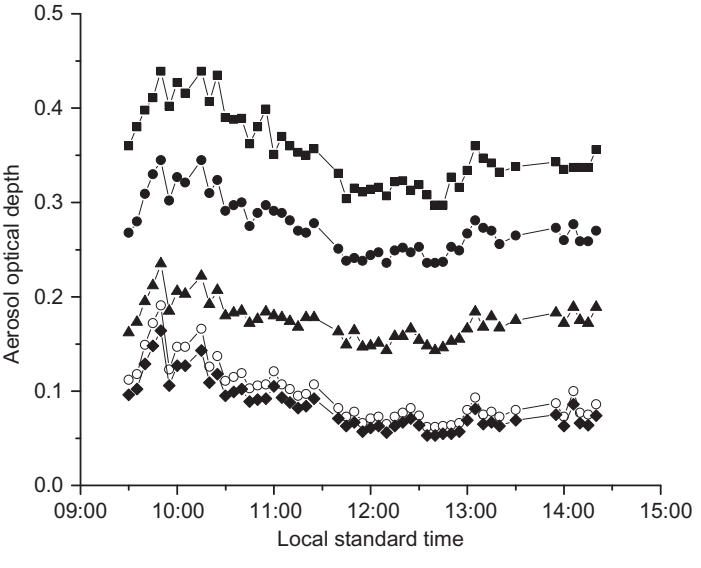

Figure 10. Daily variation of the aerosol optical depth at wavelengths $\lambda = 380$ nm (squares), $\lambda = 500$ nm (filled circles), $\lambda = 675$ nm (filled triangles), $\lambda = 936$ nm (unfilled circles) and $\lambda = 1020$ nm (filled rhombs) obtained by sun photometer on 22 May 2009 at the Astronomical Observatory, Sofia.

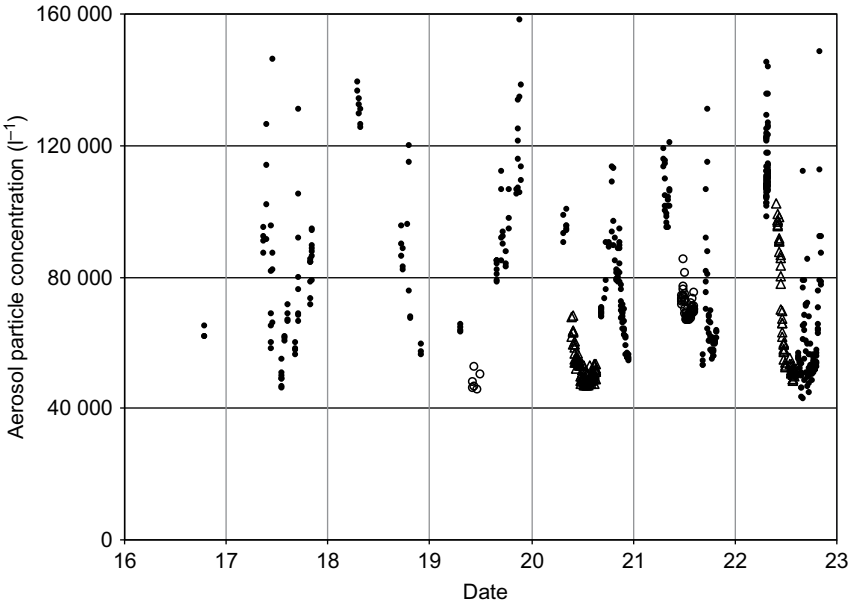

Figure 11. Daily variation (GMT+3) of aerosol particle concentration (number per litre, in size range 0.3–1 μm) measured in Sofia by aerosol particle counter over the period 16–22 May 2009. Filled circles denote data from residential area around 100 m from high traffic road; unfilled circles denote data from the Plana Observatory Site; unfilled triangles denote data from the Sofia Observatory Site.

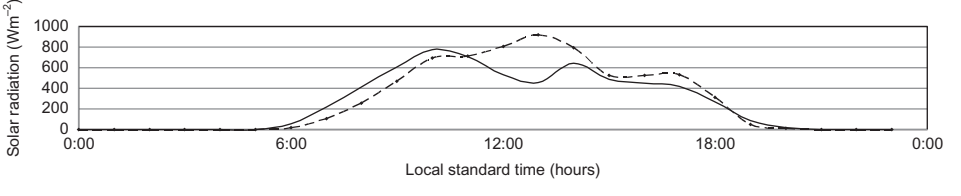

Figure 12. Daily variation of solar radiation obtained by meteorological station on 21 May 2009. Solid line, Plana Mountain site; dashed line, city park site at the Astronomical Observatory, Sofia.

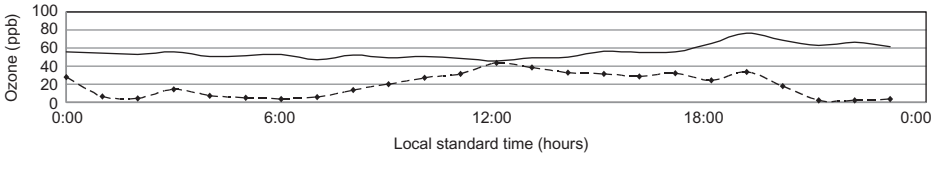

Figure 13. Daily variation of ozone concentration obtained by meteorological station on 21 May 2009. Solid line, Plana Mountain site; dashed line, city park site at the Astronomical Observatory, Sofia.

ozone concentrations at the sites is shown in figure 13. In the mountain region, the temperature varied from 12°C in the morning to 21°C in the afternoon. The relative humidity varied from 80% in the morning to 50% in the afternoon. The wind

speed was from 1.4 to 0.4 m s^{-1} and a few maxima were observed during the day. The maximum of solar radiation varied in the range 600–900 W m^{-2} and the variations were higher than those at AO. At the AO site, the temperature varied from 16°C in the morning to 26°C in the afternoon. The relative humidity varied from 95% in the morning to 40% in the afternoon. The wind speed was from 0.2 to 0.6 m s^{-1}. The maximum of solar radiation in that period varied in the range 600–900 W m^{-2}.

At the CGS site, the ground-near ozone concentration was almost constant until around 12:00 LST, then began to increase towards a maximum around 19:00 LST when the solar radiation is low. This is an evidence for ozone transport from other regions. The ground ozone concentration at the AO site reached the values obtained in the Plana Mountain after 12:00 LST and started to decrease due to low solar radiation and processes in the ML in the afternoon hours.

Solar radiation measured at the CGS and AO sites on 22 May 2009 is shown in figure 14, and the ground-near ozone concentration variations at the sites are shown in figure 15. Temperatures at the Plana site varied from 8°C in the morning to between 21 and 25°C in the afternoon. The relative humidity varied from 98% in the morning to 38% in the afternoon; wind speeds ranged from 0.8 to 3 m s^{-1} and a few maxima were observed during the day. The maximum of solar radiation varied in the range 600–1000 W m^{-2}; variations were higher than those at the AO site. The ground-near ozone concentrations varied more slowly than at AO and were between 40 and 60 ppb.

At the AO site, temperature varied from 10°C in the morning to 30°C in the afternoon; relative humidity varied from 98% in the morning to 30% in the afternoon, and is inversely related to temperature. The wind speed was from 0.1 to 0.6 m s^{-1}. The maximum of solar radiation in that period varied slowly in the range 900–980 W m^{-2}. Ground-near ozone concentrations were in the range from 10 ppb (morning hours) to 45 ppb (noon).

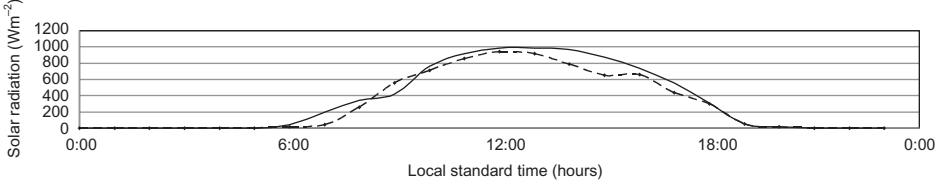

Figure 14. Daily variation of solar radiation obtained by meteorological station on 22 May 2009. Solid line, Plana Mountain site; dashed line, city park site at the Astronomical Observatory, Sofia.

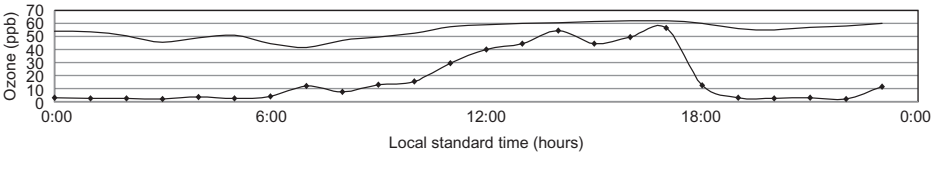

Figure 15. Daily variation of ozone concentration obtained by meteorological station on 22 May 2009. Solid line, Plana Mountain site; dashed line, city park site at the Astronomical Observatory, Sofia.

4.4 *Comparison between the lidar data and model calculations*

Figure 16 shows the comparison between the evolutions in time of the ML determined from the lidar data obtained on 5 September 2008 and the one calculated following the model of Whitman and McKee (1982). A relatively good agreement between experiment and theory is obtained when assigning the value 1 to the parameter k (which determines the ML manner of formation and rate of development and the RL rate of subsidence). When $k = 0$, the equations provide an approximate simulation of inversion destruction due solely to the removal of air mass from a valley by the slope flows, resulting in a descent of the inversion top. When $k = 1$, the equations provide a simulation of inversion destruction in which the destruction occurs mainly due to the growth of a CBL over the valley floor. When $k = 0$ and the valley floor becomes very wide, the simulation approaches that of inversion destruction over plains. When k is between 0 and 1, the equations provide a simulation of inversion destruction in which the inversion is destroyed by the combined effect of growing CBL and a descending inversion top. The maximum of incoming insolation at the Earth's surface is 900 W m^{-2}. Figure 16 suggests that at 10:30 LST the MLH determined from the lidar data is almost identical to the one obtained from the model calculations. The mean rate of ML development is 140 m hour^{-1}. After this period and up to 13:00 LST, significant fluctuations occur in the MLH determined from the lidar data. In spite of this, a relatively good model approximation of the experimental data is obtained.

In figure 17 we compare the changes in ML and RL heights in time determined from the lidar data obtained on 21 May 2009 vis-à-vis those calculated by the model. Assigning the value 0.4 to the parameter k (Whiteman and McKee 1982) results in a relatively good agreement between experimental and model results for the rate of development of the ML, the rate of subsidence of the RL, the height where these two layers reach each other and the duration of the process of ML development.

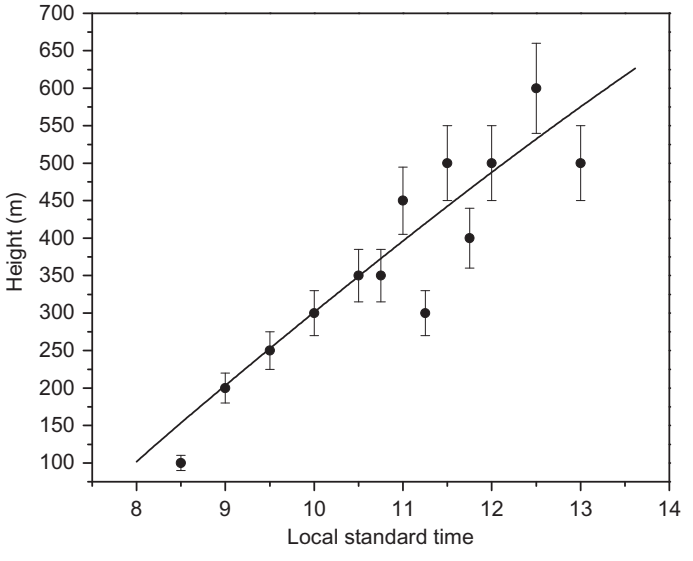

Figure 16. Comparison between lidar (filled circles) and model (solid line) data for the mixing layer height on 5 September 2008.

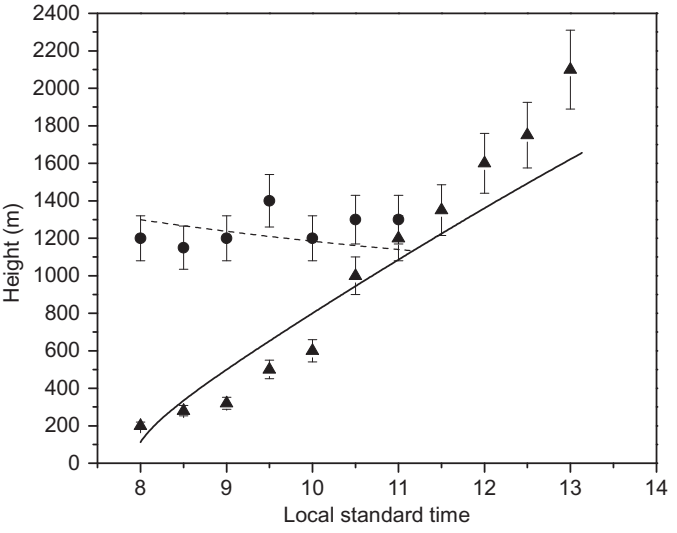

Figure 17. Comparison between lidar (triangles, mixing layer (ML) top; filled circles, residual layer (RL) bottom) and model (solid line, ML top; dashed line, RL bottom) data for the ML and RL heights on 21 May 2009.

The maximum of the insolation value at the Earth's surface is 800 W m^{-2}. Significant fluctuations in the heights determined from the lidar data are observed during the RL subsidence. The best agreement between the experimental and model data is obtained when assigning a value around 35 m $hour^{-1}$ to the rate of subsidence in the model.

Concerning the ML development, however, certain dephasing between the lidar and model data is observed. In contrast to the model which predicts an almost linear increase in the ML at a rate of 400 m $hour^{-1}$, the lidar data point to a significant delay in the development of this layer in the period from 08:30 LST to 10:00 LST. The increase observed at the ML upper boundary in this period is also almost linear, but the rate is significantly lower about 200 m $hour^{-1}$. A very rapid rise of the ML at a rate of 600 m $hour^{-1}$ (figure 17) is observed after 10.00 LST. The ML reaches a height of about 1300 m at 11:30 LST and merges and destroys the sinking RL. After that, the ML rises up to 2200 m according to the lidar data.

The delay observed in the ML development in the period from 08:30 to 10:00 LST could be due to the fact that at that time the solar radiation feeds two processes, one being the development of ML and the other representing the removal of heated air flows upwards along the slopes of the adjoining mountain range (Vitosha). This, in turn (due to the law of conservation of mass), leads to subsidence of the RL. Furthermore, the formation of multilayered temperature inversions in the morning hours before sunrise is characteristic of the region as the first elevated inversion layer is at a height between 200 and 400 m. The destruction of this layer requires significantly more energy for the development of ML in comparison with neutral stratification which, in turn, causes additional delay in the ML development. After the inversion layer destruction, the energy loss for ML development is not so high and the ML begins to grow considerably faster.

5. Discussion and summary

In this article, focusing on a heavily urbanized mountain valley (the Sofia city basin), we have presented campaign-based measurements of the structure of aerosol layers, aerosol optical characteristics and aerosol number concentrations. Our measurements employed a ground-based backscattering lidar, a commercial five-channel handheld sun photometer, a ceilometer, an LPC and meteorological stations that included ozonemeters. It merits special mention that new instruments were used for the first time in Bulgaria during this complex experiment. First, the inclusion of ceilometer CHM 15k constitutes a novel component. It enables observation of the aerosol structure of the atmosphere up to the tropopause which is important when assessing the influence of high clouds on ABL development. Second, the use of an LPC enabled us to address the aerosol particle number concentration variations and the particle size distributions. Third, three-point measurements were carried out in the valley of Sofia for the first time: at the IE site (lidar and ozonemeter), in the Borisova Gradina Park (AO site) (ceilometer, meteostation, sun photometer and LPC) and on the Plana Mountain (CGS site) (meteostation, ozonemeter and LPC).

We have presented and discussed the data from the different devices separately, and also have addressed several aspects on the joint interpretation of these data. Taken together, we believe the results constitute an important step towards understanding several crucial issues (including scattering of solar irradiation; cloud formation; local/regional climate change; health effects) pertaining to a large city situated in a mountain valley.

The ceilometer data enabled us to assess the influence of the whole atmospheric layer up to the tropopause on the ABL development in the valley of Sofia (e.g. the experimental data on 15 May 2009). Comparisons between the lidar data for the ML height in the region of IE and the ceilometer data for the ML height above the AO site showed that the ML in the region of AO developed with a delay of about 1–1.5 hours compared with the formation of the ML in the region of IE, in particular with reference to the time point when ML reaches its maximum height. The maximum height of the ML in the region of AO in some cases is 100–200 m greater than the one measured in the region of IE. In contrast to the lidar data, the ceilometer data can be obtained continuously over 24 hours, which enabled us to follow the ML destruction dynamics as well as the formation of the RL and SBL after sunset. This highlights the advantage of lidars such as the ceilometer CHM 15k used in our study.

Joint interpretation of sun photometer, aerosol lidar and ceilometer data enabled assessments of the influence of the main part of the atmospheric aerosol in the ABL as well as the significant influence on AOD values by aerosol layers and high clouds located in the tropopause-near region. Measurements of AOD gave values in the range 0.22–0.41 for cloud-free skies, and up to around 0.80 under partly cloudy conditions. LPC data on aerosol particle concentration variations in the size range 0.3–1 μm provided supportive information on the evolution of the valley–mountain aerosol in time and height during the ML development. In general, higher aerosol particle concentration values were obtained in the urban region (Sofia city basin) in comparison with those obtained at the Plana Mountain that forms a part of the mountain ranges that surround the city basin. Particle number concentrations in the size range 0.3–1 μm varied strongly in the Sofia basin, with high concentrations fairly concomitant with morning and afternoon road traffic peaks and with the formation of inversion layers.

From the above observations, we have found that our lidar-based field data on the dynamics of the ML compare favourably with results from models of such dynamics.

When the maximum height of ML is reached, all of the conservative atmospheric components should be the same in the whole layer. Figure 15 clearly shows that the ground-near ozone concentration in the city basin approaches the values occurring in the Plana Mountain (around 600 m above the basin) around noon. There is a similar relation between the ground ozone concentration measured in AO and the one measured at the 'Kopitoto' Station at 1350 m above sea level at the northwestern side of Vitosha Mountain.

In conclusion, our study demonstrates the potential of employing a broad array of instruments for the study of boundary layer and aerosol and ozone dynamics over large, valley-situated and heavily urbanized city areas. In particular, experimental set-ups will be needed that include instruments of the types that are addressed in this article and that enable concomitant measurements, over time, in and above the city basin. Such arrangements will also assist in testing hypotheses with respect to spatial homogeneity of atmospheric pollution in the case of fully developed ML over an urban area in a mountain valley, and with respect to local to regional climate change.

Acknowledgements

This work was carried out within the project 'City versus Mountain Tropospheric Ozone: The Sofia-Plana region in an air quality and ecological sustainability perspective' (contract DO 02-127/08). Parts of the lidar results are within the framework of the Atmospheric Composition Change: the European Network (ACCENT) and European Aerosol Research Lidar Network – Advanced Sustainable Observation System (EARLINET-ASOS) Project. LPC measurements were partly funded by the Kalmar University Faculty of Natural Science and Technology.

References

Alados-Arboledas, L., Alcantara, A., Olmo, F.J., Martinez-Lozano, J.A., Estelles, V., Cachorro, V., Silva, A.M., Horvath, H., Gangl, M., Diaz, A., Pujadas, M., Lorente, J., Labajo, A., Sorribas, M. and Pavese, G., 2008, Aerosol columnar properties retrieved from Cimel radiometry during Veleta 2002. *Atmospheric Environment*, **42**, pp. 2654–2667.

Alfoldy, B., Osan, J., Toth, Z., Torok, S., Harbusch, A., Jahn, C., Emeis, S. and Schafer, K., 2007, Aerosol optical depth, aerosol composition and air pollution during summer and winter conditions in Budapest. *Science of the Total Environment*, **383**, pp. 141–163.

Beyrich, F., Ackrr, K., Kalas, D., Klemm, O., Moller, D., Eschaller, E., Werhahn, J. and Weisensee, U., 1996a, Boundary layer structure and photochemical pollution in the Harz Mountains – an observational study. *Atmospheric Environment*, **30**, pp. 1271–1281.

Beyrich, F., Weisensee, U., Sprung, D. and Gusten, H., 1996b, Comparative analysis of sodar and ozone profile measurements in a complex structured boundary layer and implications for mixing height estimation. *Boundary-Layer Meteorology*, **81**, pp. 1–9.

Cartalis, C. and Varotsos, C., 1994, Surface ozone in Athens, Greece, at the beginning and at the end of 20th-century. *Atmospheric Environment*, **28**, pp. 3–8.

Chandra, S. and Varotsos, C.A., 1995, Recent trends of the total column ozone: implications for the Mediterranean region. *International Journal of Remote Sensing*, **16**, pp. 1765–1769.

Chou, C.C.-K., Lee, C.-T., Chen, W.-N., Chang, S.-Y., Chen, T.-K., Lin, C.-Y. and Chen, J.-P., 2007, Lidar observation of the diurnal variations in the depth of urban mixing layer: a case study on the air quality deterioration in Taipei, Taiwan. *Science of the Total Environment*, **374**, pp. 156–166.

Collis, R.T.H. and Russell, P.B., 1976, Lidar measurements of particles and gases by elastic backscattering and differential absorption. In *Laser Monitoring of the Atmosphere*, E.D. Hinkley (Ed.), pp. 71–151 (New York: Springer).

Cracnell, A.P. and Varotsos, C.A., 2007, The IPCC fourth assessment report and the fiftieth anniversary of Sputnik. *Environmental Science and Pollution Research*, **14**, pp. 384–387.

Devara, P.C.S., Pandithurai, G., Raj, P.E. and Sharma, S., 1996, Investigations of aerosol optical depth variations using spectroradiometer at an urban station, Pune, India. *Journal of Aerosol Science*, **27**, pp. 621–632.

Donev, E., Zeller, K. and Avramov, A., 2002, Preliminary background ozone concentrations in the mountain and coastal areas of Bulgaria. *Environmental Pollution*, **117**, pp. 281–286.

Evgenieva, Ts.T, Kolev, N., Iliev, I., Savov, P., Kaprielov, B., Devara, P.C.S. and Kolev, I., 2009, Lidar and spectroradiometer measurements of the atmospheric aerosol optical characteristics over urban area (Sofia, Bulgaria). *International Journal of Remote Sensing*, **30**, pp. 6381–6401.

Fenger, J., 2009, Air pollution in last 50 years – from local to global. *Atmospheric Environment*, **43**, pp. 13–22.

Ferm, M., De Santis, F. and Varotsos, C., 2005, Nitric acid measurements in connection with corrosion studies. *Atmospheric Environment*, **39**, pp. 6664–6672.

Ferm, M., Watt, J., O'hanlon, S., De Santis, F. and Varotsos, C., 2006, Deposition measurement of particulate matter in connection with corrosion studies. *Analytical and Bioanalytical Chemistry*, **384**, pp. 1320–1330.

Gerasopoulos, E., Kouvarakis, G., Vrekoussiss, M., Kanakidou, M. and Mihalopoulos, N., 2005, Ozone variability in the marine boundary layer of the eastern Mediterranean based on 7-year observations. *Journal of Geophysical Research*, **110**, D15309.

Gernandt, H., Goersdorf, U., Claude, H. and Varotsos, C.A., 1995, Possible impact of polar stratospheric processes on mid-latitude vertical ozone distributions. *International Journal of Remote Sensing*, **16**, pp. 1839–1850.

Grimmod, C.S.B., 2006, Progress in measuring and observing the urban atmosphere. *Theoretical and Applied Climatology*, **84**, pp. 3–22.

Guerrero-Rascado, J.L., Olmo, F., Aviles-Rodriguez, I., Navas-Guzman, F., Perez-Ramirez, D., Lyamani, H. and Alados-Arboledas, L., 2009, Extreme Saharan dust event over the Southern Iberian Peninsula in September 2007: active and passive remote sensing from surface and satellite. *Atmospheric Chemistry and Physics*, **9**, pp. 8453–8469.

Hongbin, Yu., Liu, S.C. and Dickinson, R.E., 2002, Radiative effects of aerosol on the evolution of the atmospheric boundary layer. *Journal of Geophysical Research*, **107**, D12, 4142, 10.1029/2001/D000754.

Houthuijs, D., Breugelmans, O., Hoel, G., Vaskövi, E., Mihailikova, E., Pastuszka, J.S., Jirik, V., Sachelarescu, S., Lolova, D., Meliefste, K., Uzunova, V., Marinescu, C., Volf, J., De Leuw, F., Van Den Wiel, H., Fletcher, T., Lebret, E. and Brunekeef, B., 2001, PM10 and PM2.5 concentrations in Central and Eastern Europe: results from the Cesar study. *Atmospheric Environment*, **35**, pp. 2757–2771.

Intergovernmental Panel on Climate Change (IPCC), 2007, Climate change 2007. In *The Physical Science Basis: Contribution of Working Group I to the Fourth Assessment Report of the Intergovernmental Panel of Climate Change*, S. Solomon, D. Qin, M. Manning, Z. Chen, M. Marquis, K.B. Averyt, M. Tignor and H.L. Miller (Eds.) (Cambridge: Cambridge University Press).

Jacob, D. and Winner, D., 2009, Effect of climate change on air quality. *Atmospheric Environment*, **43**, pp. 51–63.

Jacovides, C.P., Varotsos, C., Kaltsounides, N.A., Petrakis, M. and Lalas, D.P., 1994, Atmospheric turbidity parameters in the highly polluted site of Athens basin. *Renewable Energy*, **4**, pp. 465–470.

KATSAMBAS, A., VAROTSOS, C.A., VEZIRYIANNI, G. and ANTONIOU, C., 1997, Surface solar ultraviolet radiation: a theoretical approach of the SUVR reaching the ground in Athens, Greece. *Environmental Science and Pollution Research*, **4**, pp. 69–73.

KOLEV, I., SAVOV, P., KAPRIELOV, B., PARVANOV, O. and SIMEONOV, V., 2000, Lidar observation of the nocturnal boundary layer formation over Sofia, Bulgaria. *Atmospheric Environment*, **34**, pp. 3223–3235.

KOLEV, N., GRIGOROV, I., KOLEV, I., DEVARA, P.C.S., RAJ, P.E. and DANI, K.K., 2007, Lidar and sun photometer observations of atmospheric boundary-layer characteristics over an urban area. *Boundary-Layer Meteorology*, **124**, pp. 99–115.

KOLEV, N., TATAROV, B., KAPRIELOV, B. and KOLEV, I., 2004, Investigation of the aerosol structure over an urban area using a polarization lidar. *Journal of Environmental Monitoring*, **19**, pp. 834–840.

KONDRATYEV, K.Y. and VAROTSOS, C., 1995, Atmospheric greenhouse effect in the context of global climate change. *Nuovo Cimento della Societa Italiana Di Fisica C – Geophysics and Space Physics*, **18**, pp. 123–151.

KONDRATYEV, K.Y. and VAROTSOS, C., 2002, Remote sensing and global tropospheric ozone observed dynamics. *International Journal of Remote Sensing*, **23**, pp. 159–178.

LYAMANI, H., OLMO, F.J. and ALADOS-ARBOLEDAS, L., 2004, Long-term changes in aerosol radiative properties at Armilla (Spain). *Atmospheric Environment*, **38**, pp. 5935–5943.

LYAMANI, H., OLMO, F.J. and ALADOS-ARBOLEDAS, L., 2005, Saharan dust outbreak over southeastern Spain as detected by sun photometer. *Atmospheric Environment*, **39**, pp. 7276–7284.

LYAMANI, H., OLMO, F.J. and ALADOS-ARBOLEDAS, L., 2008, Light scattering and absorption properties of aerosol particles in the urban environment of Granada, Spain. *Atmospheric Environment*, **42**, pp. 2630–2642.

LYAMANI, H., OLMO, F.J., ALCANTARA, A. and ALADOS-ARBOLEDAS, L., 2006a, Atmospheric aerosols during the 2003 heat wave in southeastern Spain I: spectral optical depth. *Atmospheric Environment*, **40**, pp. 6453–6464.

LYAMANI, H., OLMO, F.J., ALCANTARA, A. and ALADOS-ARBOLEDAS, L., 2006b, Atmospheric aerosols during the 2003 heat wave in southeastern Spain II: microphysical columnar properties and radiative forcing. *Atmospheric Environment*, **40**, pp. 6465–6476.

MARKOWICZ, K., FLATAN, P., QUINN, P., CARRICO, C., FALATAN, M., VOGELMANN, A., BATES, D., LIN, M. and ROOD, M., 2003, Influence of relative humidity on aerosol radiative forcing: an ACE-Asia experiment perspective. *Journal of Geophysical Research*, **108**, p. 8662.

MARTINEZ-LOZANO, J.A., UTRILLAS, M.P., TENA, F. and CACHORRO, V.E., 1998, The parameterisation of the atmospheric aerosol optical depth using the Angstrom power law. *Solar Energy*, **63**, pp. 303–311.

MCKENDRY, I.G., VAN DER KAMP, D., STRAWBRIDGE, K.B., CHRISTEN, A. and CRAWFORD, B., 2009, Simultaneous observations of boundary layer aerosol layers with CL31 ceilometer and 1064/532 lidar. *Atmospheric Environment*, **43**, pp. 5847–5852.

MEDEIROS, B., HALL, A. and STEVENS, B., 2005, What control the mean depth of the PBL? *Journal of Climate*, **18**, pp. 3157–3172.

REINAP, A., WIMAN, B.L.B., SVENNINGSSON, B. and GUNNARSSON, S., 2009, Oak leaves as aerosol collectors: relationships with wind velocity and particle size distribution. Experimental results and their implications. *Trees*, **23**, pp. 1263–1274.

SAVOV, P., SKAKALOVA, T., KOLEV, I. and LUDWIG, F.L., 2002, Lidar investigation of the temporal and spatial distribution of atmospheric aerosols in mountain valley. *Journal of Applied Meteorology*, **41**, pp. 528–541.

SEIBERT, P., BEYRICH, F., GRYNING, S.-E., JOFFE, S., RASMUSSEN, A. and TERCIER, PH., 2000, Review and intercomparison on operational methods for the determination of mixing height. *Atmospheric Environment*, **34**, pp. 1001–1027.

Seinfeld, J.H. and Pandis, S.N., 1998, *Atmospheric Chemistry and Physics. from Air Pollution to Climate Change* (New York: John Wiley & Sons).

Sicard, M., Perez, C., Rocadenbosch, F., Baldasano, J.M. and Garcia-Vizcaino, D., 2006, Mixed-layer depth determination in the Barcelona Coastal area from regular lidar measurements: methods, results and limitations. *Boundary-Layer Meteorology*, **119**, pp. 135–157.

Tzanis, C. and Varotsos, C.A., 2008, Tropospheric aerosol forcing of climate: a case study for the greater area of Greece. *International Journal of Remote Sensing*, **29**, pp. 2507–2517.

Varotsos, C., 2004, Atmospheric pollution and remote sensing: implications for the southern hemisphere ozone hole split in 2002 and the northern mid-latitude ozone trend, Monitoring of Changes Related to Natural and Manmade Hazards Using Space Technology. *Advances in Space Research*, **33**, pp. 249–253.

Varotsos, C., Cartalis, C., Vlamakis, A., Tzanis, C. and Keramitsoglou, I., 2004, The long-term coupling between column ozone and tropopause properties. *Journal of Climate*, **17**, pp. 3843–3854.

Varotsos, C., Kondratyev, K.Y. and Efstathiou, M., 2001a, On the seasonal variation of the surface ozone in Athens, Greece. *Atmospheric Environment*, **35**, pp. 315–320.

Varotsos, C.A., Alexandris, D., Chronopoulos, G. and Tzanis, C., 2001b, Aircraft observations of the solar ultraviolet irradiance throughout the troposphere. *Journal of Geophysical Research-Atmospheres*, **106**, pp. 14843–14854.

Varotsos, C.A., Chronopoulos, G.J., Katsikis, S. and Sakellariou, N.K., 1995, Further evidence of the role of air-pollution on solar ultraviolet-radiation reaching the ground. *International Journal of Remote Sensing*, **16**, pp. 1883–1886.

Velasco, E., Marquez, C., Bueno, E., Bernabe, R., Sanchez, A., Fentanes, O., Wohrnschimmel, H., Cardenas, B., Kamilla, A., Wakamatsu, S. and Molina, L., 2008, Vertical distribution of ozone and VOCs in the low boundary layer of Mexico City. *Atmospheric Chemistry and Physics*, **8**, pp. 3061–3079.

Whitby, K.T., 1978, The physical characteristics of sulfur aerosols. *Atmospheric Environment*, **12**, pp. 135–161.

Whiteman, C.D. and McKee, T.B., 1982, Breakup of temperature inversions in deep mountain valleys: part II, thermodynamic model. *Journal of Applied Meteorology*, **21**, pp. 290–302.

Wiman, B.L.B., Donev, E.H., Nikolova, P.N. and Yurukova, L.D., 2007, Aerosol-borne trace elements in Bulgaria: concentration levels in coastal and mountainous regions. *Bulgarian Geophysical Journal*, **33**, pp. 3–19.